

# Diff-IP2D: Diffusion-Based Hand-Object Interaction Prediction on Egocentric Videos

Junyi Ma<sup>1</sup>, Xieyuanli Chen<sup>2</sup>, Jingyi Xu<sup>3</sup>, Hesheng Wang<sup>1\*</sup>

**Abstract**—Understanding how humans would behave during hand-object interaction (HOI) is vital for applications in service robot manipulation and extended reality. To achieve this, some recent works simultaneously forecast hand trajectories and object affordances on human egocentric videos. The joint prediction serves as a comprehensive representation of future HOI in 2D space, indicating potential human motion and motivation. However, the existing approaches mostly adopt the autoregressive paradigm, which lacks bidirectional constraints within the holistic future sequence, and accumulates errors along the time axis. Meanwhile, they overlook the effect of camera egomotion on first-person view predictions. To address these limitations, we propose a novel diffusion-based HOI prediction method, namely Diff-IP2D, to forecast future hand trajectories and object affordances with bidirectional constraints in an iterative non-autoregressive manner on egocentric videos. Motion features are further integrated into the conditional denoising process to enable Diff-IP2D aware of the camera wearer’s dynamics for more accurate interaction prediction. Extensive experiments demonstrate that Diff-IP2D significantly outperforms the state-of-the-art baselines on both the off-the-shelf and our newly proposed evaluation metrics. This highlights the efficacy of leveraging a generative paradigm for 2D HOI prediction. The code of Diff-IP2D will be released as open source at <https://github.com/IRMVLab/Diff-IP2D>.

## I. INTRODUCTION

Accurately anticipating human intentions and future actions is important for artificial intelligence systems in robotics and extended reality [1]–[3]. Recent works have tried to tackle the problem from various perspectives, including action recognition and anticipation [4]–[7], gaze prediction [8]–[11], hand trajectory prediction [12]–[15], and object affordance extraction [12], [14], [16], [17]. Among them, jointly predicting hand motion and object affordances can effectively facilitate more reasonable robot manipulation as the prior contextual information, which has been demonstrated on some robot platforms [1], [18], [19]. We believe that deploying such models pretrained by internet-scale human videos on robots is a promising path towards embodied agents. Therefore, our work aims to jointly predict hand trajectories and object affordances on egocentric videos as a concrete hand-object interaction (HOI) expression, following the problem modeling of previous works [12], [14].

Currently, the state-of-the-art approaches [12], [13] predicting hand trajectories and object affordances on egocentric

<sup>1</sup>Junyi Ma and Hesheng Wang are with IRMV Lab, the Department of Automation, Shanghai Jiao Tong University, Shanghai 200240, China.

<sup>2</sup>Xieyuanli Chen is with the College of Intelligence Science and Technology, National University of Defense Technology, Changsha 410073, China.

<sup>3</sup>Jingyi Xu is with the Department of Electronic Engineering, Shanghai Jiao Tong University, Shanghai 200240, China.

\*Corresponding author email: wanghesheng@sjtu.edu.cn

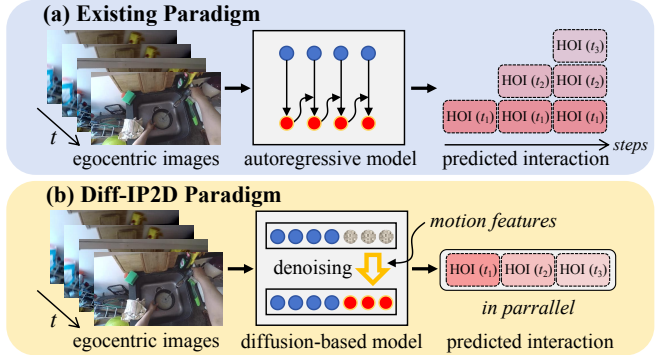


Fig. 1: Diff-IP2D vs. Existing Paradigm. The existing HOI prediction paradigm (a) tends to accumulate prediction errors under unidirectional constraints. In contrast, our proposed Diff-IP2D (b) directly forecasts all future HOI states in parallel with denoising diffusion, mitigating error accumulation with bidirectional constraints.

videos tend to exploit the autoregressive (AR) model. They reason about the next HOI state only according to the previous steps (Fig. 1(a)). However, expected “post-contact states” also affect “pre-contact states” according to human intentions that persist across the holistic HOI process as an oracle. Inspired by this, we argue that predicting future HOI states in parallel considering the bidirectional constraints within the holistic sequence outperforms generating the next state autoregressively. With diffusion models emerging across multiple domains [20]–[27], their strong forecasting capability has been widely validated. Therefore, we propose a diffusion-based method to predict future hand-object interaction in parallel, considering bidirectional constraints in the latent space compared to the traditional autoregressive generation (Fig. 1(b)).

Moreover, we also identify two inherent gaps affecting HOI prediction in the existing paradigm: 1) Directly predicting the projection of 3D future hand trajectories and object affordances on 2D egocentric image plane is an ill-posed problem involving spatial ambiguities. There is generally a gap between 2D pixel movements and 3D real actions, which can be bridged by spatial transformation across multiple views changing with egomotion. 2) The past egocentric videos are absorbed to predict future interaction states on the last observed image, which is actually a “canvas” from a different view w.r.t all the other frames. Therefore, there is also a gap between the last observation (egocentric view) and the other observations (analogous to exocentric view) caused by egomotion. To fill the two gaps together, we further propose to integrate the camera wearer’s egomotion into our diffusion-based paradigm. It enables the denoising model aware of the camera wearer’s dynamics and the spatial

relationship between consecutive frames.

The main contributions of this paper are as follows: 1) We propose a diffusion-based hand-object interaction prediction method, dubbed Diff-IP2D. To our best knowledge, this is the first work using the devised denoising diffusion probabilistic model to jointly forecast future hand trajectories and object affordances with only 2D egocentric videos as input. It provides a foundation generative paradigm in the field of HOI prediction. 2) The homography egomotion features are integrated to fill the motion-related gaps inherent in HOI prediction on egocentric videos. 3) We extend the existing metrics and propose the first protocol for jointly evaluating the performance of hand trajectory prediction and object affordance prediction. Comprehensive experiments are conducted to demonstrate that our Diff-IP2D can predict better hand trajectories and object affordances compared to the state-of-the-art baselines, showing its potential for deployment on artificial intelligence systems.

## II. RELATED WORK

**Understanding hand-object interaction.** Human HOI comprehension can guide the downstream tasks in artificial intelligence systems. Calway et al. [28] and Liu et al. [29] both innovatively connect human tasks to relevant objects, which underlines the relationship between object-centric interaction and goal-oriented human activities. After that, many works contribute to HOI understanding by pixel-wise segmentation [30]–[33], bounding-box-wise detection [15], [34]–[36], fine-grained hand/object pose estimation [37]–[42]. Ego4D [43] further provides a standard benchmark that divides HOI understanding into several predefined subtasks.

**Predicting hand-object interaction.** Analyzing only past human behavior may be insufficient for service robot manipulation or extended reality. Forecasting possible future object-centric HOI states based on historical observations is also valuable, which attracts increasing attention due to the general knowledge that can be transferred to robot applications [1], [18], [19], [44]. For example, Dessalene et al. [45] propose to generate contact anticipation maps and next active object segmentations as future HOI predictions. Liu et al. [14] first achieve hand trajectory and object affordance prediction simultaneously, revealing that predicting hand motion benefits the extraction of interaction hotspots, and vice versa. Following this work, Liu et al. [12] further develop an object-centric Transformer to jointly forecast future trajectories and affordances autoregressively, and annotate publicly available datasets to support future works. More recently, Bao et al. [13] lift the problem to 3D spaces where hand trajectories are predicted by an uncertainty-aware state space Transformer in an autoregressive manner. However, it needs additional 3D perception inputs from the RGB-D camera. In this work, we still achieve joint hand trajectory and object affordance prediction on 2D human videos rather than in 3D space. We focus on capturing more general knowledge from only egocentric 2D observations in an iterative non-autoregressive (iter-NAR) manner, rather than the autoregressive way of the state-of-the-art works [12], [13].

**Diffusion-based egocentric video analysis.** Diffusion models have been successfully utilized in some egocentric vision tasks due to their strong generation ability, such as video prediction [2], [46], human mesh recovery [47], [48], 3D HOI reconstruction [49], [50], and 3D HOI synthesizing [16], [51]. However, none of these works concentrate on the combination of fine-grained hand trajectories and object affordances as future HOI representations for potential utilization in artificial intelligence systems. Our Diff-IP2D first achieves this based on the denoising diffusion probabilistic model [20], which dominates the existing paradigm [12], [13] in prediction performance on egocentric videos.

## III. PROPOSED METHOD

### A. Preliminaries

**Task definition.** Given the video clip of past egocentric observations  $\mathcal{I} = \{I_t\}_{t=-N_p+1}^0$ , we aim to predict future hand trajectories  $\mathcal{H} = \{H_t^R, H_t^L\}_{t=1}^{N_f} (H_t^R, H_t^L \in \mathbb{R}^2)$  and potential object contact points  $\mathcal{O} = \{O_n\}_{n=1}^{N_o} (O_n \in \mathbb{R}^2)$ , where  $N_p$  and  $N_f$  are the numbers of frames in the past and future time horizons respectively, and  $N_o$  denotes the number of predicted contact points used to calculate interaction hotspots as object affordances. Following the previous works [12], [14], we predict the future positions of the right hand, the left hand, and the affordance of the next active object on the last observed image of the input videos as a canvas.

**Diffusion models.** In this work, we propose a diffusion-based approach to gradually corrupt the input to noisy features and then train a denoising model to reverse this process. We first map the input images into a latent space  $\mathbf{z}_0 \sim q(\mathbf{z}_0)$ , which is then corrupted to a standard Gaussian noise  $\mathbf{z}_s \sim \mathcal{N}(0, \mathbf{I})$ . In the forward process, the perturbation operation can be represented as  $q(\mathbf{z}_s | \mathbf{z}_{s-1}) = \mathcal{N}(\mathbf{z}_s; \sqrt{1 - \beta_s} \mathbf{z}_{s-1}, \beta_s \mathbf{I})$ , where  $\beta$  is the predefined variance scales. In the reverse process, we set a denoising diffusion model to gradually reconstruct the latent  $\mathbf{z}_0$  from the noisy  $\mathbf{z}_s$ . The denoised features can be used to recover the final future hand trajectories and object affordances.

### B. Architecture

**System overview.** Accurately reconstructing the future part of the input sequence is critical in diffusion-based prediction. We found that ground-truth hand waypoints  $\mathcal{H}^{gt} = \{H_t^{R,gt}, H_t^{L,gt}\}_{t=1}^{N_f} (H_t^{R,gt}, H_t^{L,gt} \in \mathbb{R}^2)$  and contact points  $\mathcal{O}^{gt} = \{O_n^{gt}\}_{n=1}^{N_o} (O_n^{gt} \in \mathbb{R}^2)$  provide discrete and sparse supervision for reconstruction, which is not enough for capturing high-level semantics such as human intentions in the denoising process. Therefore, as Fig. 2 shows, we first use the Multi-Feature Extractor and Side-Oriented Fusion Module to transform input images into latent HOI features, and then implement diffusion-related operation in the latent continuous space. The HOI features denoised by the Motion-Aware Denoising Transformer are further absorbed by the Hand Trajectory Head and Object Affordance Head to generate future hand trajectories and object hotspots.

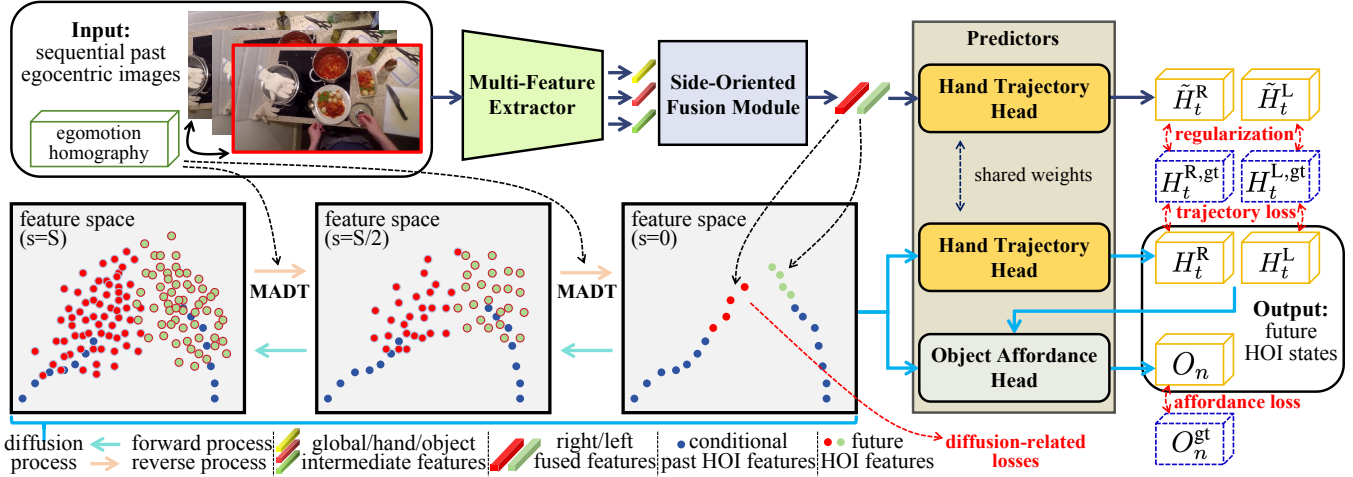


Fig. 2: System Overview of Diff-IP2D. Our proposed paradigm takes in sequential past egocentric images and jointly predicts hand trajectories and object affordances as future HOI states. The observations are mapped to the latent feature space for the diffusion process.

**Multi-Feature Extractor (MFE).** Following the previous work [12], we use MFE that consists of a pretrained Temporal Segment Network (TSN) provided by Furnari et al. [34], RoIAlign [52] with average pooling, and Multilayer Perceptron (MLP) to extract hand, object, and global intermediate features for each sequence image  $I_t \in \mathcal{I}$ . The positions of hand-object bounding boxes detected by the off-the-shelf approach [15] are also encoded to feature vectors fused with hand and object intermediate features.

**Side-Oriented Fusion Module (SOFM).** Our proposed SOFM is a learnable linear transformation to fuse the above-mentioned three types of feature vectors into the final latent form for two sides respectively. Specifically, the global features and right-side features (right-hand/object features) are concatenated to the right-side HOI features  $\mathcal{F}^R = \{F_t^R\}_{t=-N_p+1}^X (F_t^R \in \mathbb{R}^a, X = N_f \text{ for training and } X = 0 \text{ for inference})$ . The operation and feature sizes are the same as the left-side counterparts, leading to  $\mathcal{F}^L = \{F_t^L\}_{t=-N_p+1}^X$ . We further concatenate the side-oriented features along the time axis respectively to generate the input latents  $F_{\text{seq}}^R, F_{\text{seq}}^L \in \mathbb{R}^{(N_p+X) \times a}$  for the following diffusion model.

**Motion-Aware Denoising Transformer (MADT).** Our proposed MADT takes in the noisy latent HOI features and reconstructs future HOI features for the following predictors conditioned on past HOI counterparts. MADT consists of devised Transformer layers as shown in Fig. 3, thus imposing bidirectional constraints on temporal latents. Following the previous work [26], we anchor the past HOI features for both forward and reverse processes. We only impose noises and denoise at the positions of the future feature sequence. The features of the two sides are denoised using the same model, leading to  $\hat{F}_{\text{seq}}^R$  and  $\hat{F}_{\text{seq}}^L$ . In addition, egomotion guidance is proposed here to fill the gaps mentioned in Sec. I. Specifically, we first extract SIFT [53] descriptors to find the pixel correspondence between two adjacent past images in  $\mathcal{I}$ . Then we use RANSAC [54] to solve the homography matrix that maximizes the number of inliers in keypoint pairs. We accumulate the consecutive homography matrices and obtain  $M_{\text{seq}} \in \mathbb{R}^{N_p \times 3 \times 3}$  representing the camera wearer’s motion

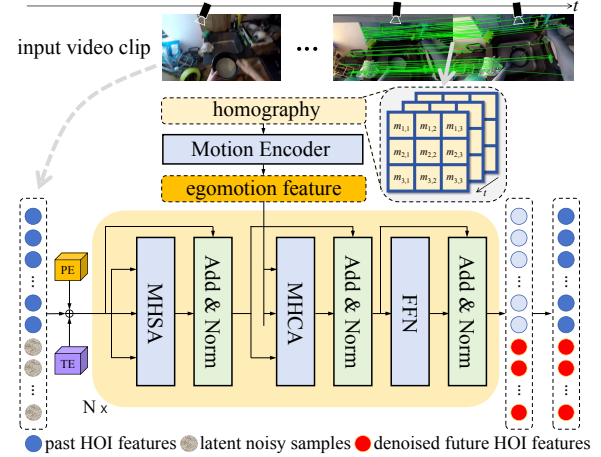


Fig. 3: Architecture of our proposed MADT. MADT receives corrupted latent HOI features with the position embedding (PE) and time embedding (TE), and outputs denoised future HOI features under the egomotion guidance.

between  $I_t (t \leq 0)$  and  $I_0$ . They are further linearly embedded into an egomotion feature  $E_{\text{seq}} \in \mathbb{R}^{N_p \times b}$  by Motion Encoder. The multi-head cross-attention module (MHCA) in MADT then absorbs the egomotion features to guide the denoising process.

**Predictors.** Our proposed predictors consist of the Hand Trajectory Head (HTH) and Object Affordance Head (OAH). HTH contains an MLP that receives the future parts of the denoised features,  $\hat{F}_{\text{seq}}^R[N_p+1:N_p+N_f]$  and  $\hat{F}_{\text{seq}}^L[N_p+1:N_p+N_f]$  to generate future waypoints  $\mathcal{H}$  of two hands. As to OAH, we empirically exploit Conditional Variational Autoencoder (C-VAE) [55] to generate possible contact points  $\mathcal{O}$  in the near future. Taking the right hand as an example, the condition is selected as the time-averaged  $\hat{F}_{\text{seq}}^R$  and predicted waypoints  $H_t^R$ . Note that we additionally consider denoised future HOI features  $\hat{F}_{\text{seq}}^R[N_p+1:N_p+N_f] (t > 0)$  besides the features from the past observation ( $t \leq 0$ ) for object affordance prediction. This aligns with the intuitive relationship between the contact points and the overall interaction process.

### C. Training

**Forward process.** We implement partial noising [26] in the forward process during training. Taking the right side as an example, the output of SOFM is first extended by a Markov transition  $q(\mathbf{z}_0|F_{\text{seq}}^{\text{R}}) = \mathcal{N}(F_{\text{seq}}^{\text{R}}, \beta_0 \mathbf{I})$ , where  $F_{\text{seq}}^{\text{R}} \in \mathbb{R}^{(N_p+N_f) \times a}$ . In each following forward diffusion step, we implement  $q(\mathbf{z}_s|\mathbf{z}_{s-1})$  by adding noise to the future part of  $\mathbf{z}_{s-1}$ , i.e.,  $\mathbf{z}_{s-1}[N_p+1:N_p+N_f]$  for both sides.

**Reverse process.** After corrupting  $\mathbf{z}_0$  to  $\mathbf{z}_S$  by the forward process, our proposed MADT is adopted to denoise  $\mathbf{z}_S$  to  $\mathbf{z}_0$ . Considering the proposed guidance of egomotion features, the reverse process can be modeled as  $p_{\text{MADT}}(\mathbf{z}_{0:S}) := p(\mathbf{z}_S) \prod_{s=1}^S p_{\text{MADT}}(\mathbf{z}_{s-1}|\mathbf{z}_s, M_{\text{seq}})$ . Specifically, the MADT model  $f_{\text{MADT}}(\mathbf{z}_s, s, M_{\text{seq}})$  predicts the injected noise for each forward step with  $p_{\text{MADT}}(\mathbf{z}_{s-1}|\mathbf{z}_s, M_{\text{seq}}) = \mathcal{N}(\mathbf{z}_{s-1}; \mu_{\text{MADT}}(\mathbf{z}_s, s, M_{\text{seq}}), \sigma_{\text{MADT}}(\mathbf{z}_s, s, M_{\text{seq}}))$ . The same denoising operation and motion-aware guidance are applied to HOI features of both sides.

**Training objective.** The loss function to train the networks in Diff-IP2D contains four parts, including diffusion-related losses, trajectory loss, affordance loss, and an additional regularization term (see Fig. 2). Taking the right side as an example, we use the variational lower bound  $\mathcal{L}_{\text{VLB}}^{\text{R}}$  as the diffusion-related losses:

$$\mathcal{L}_{\text{VLB}}^{\text{R}} = \sum_{s=2}^S \|\mathbf{z}_0^{\text{R}} - f_{\text{MADT}}(\mathbf{z}_s^{\text{R}}, s, M_{\text{seq}})\|^2 + \|F_{\text{seq}}^{\text{R}} - \hat{F}_{\text{seq}}^{\text{R}}\|^2, \quad (1)$$

where  $\hat{F}_{\text{seq}}^{\text{R}} = f_{\text{MADT}}(\mathbf{z}_1^{\text{R}}, 1, M_{\text{seq}})$ . To reconstruct hand trajectories beyond the latent feature space, we further set trajectory loss  $\mathcal{L}_{\text{traj}}^{\text{R}}$  with the distance between the ground-truth waypoints and the ones predicted by HTH:

$$\mathcal{L}_{\text{traj}}^{\text{R}} = \sum_{t=1}^{N_f} \|H_t^{\text{R}} - H_t^{\text{R},\text{gt}}\|^2, \quad (2)$$

where  $H_t^{\text{R}} = f_{\text{HTH}}(\hat{F}_{\text{seq}}^{\text{R}}[N_p+1:N_p+N_f])$ . As to the object affordance prediction, we also compute the affordance loss  $\mathcal{L}_{\text{aff}}$  after multiple stochastic sampling considering the next active object recognized following Liu et al. [12] (assuming in the right side here for brevity):

$$\mathcal{L}_{\text{aff}} = \sum_{n=1}^{N_o} \|O_n - O_n^{\text{gt}}\|^2 + c\mathcal{L}_{\text{KL}}, \quad (3)$$

where  $O_n = f_{\text{OAH}}(\hat{F}_{\text{seq}}^{\text{R}}, H_t^{\text{R}})$  is the predicted contact points, and  $\mathcal{L}_{\text{KL}} = \frac{1}{2}(-\log \sigma_{\text{OAH}}^2(\hat{F}_{\text{seq}}^{\text{R}}, H_t^{\text{R}}) + \mu_{\text{OAH}}^2(\hat{F}_{\text{seq}}^{\text{R}}, H_t^{\text{R}}) + \sigma_{\text{OAH}}^2(\hat{F}_{\text{seq}}^{\text{R}}, H_t^{\text{R}}) - 1)$  is the KL-Divergence regularization for C-VAE, which is scaled by  $c = 1e-3$ . The latent features and predicted hand waypoints are fused by MLP suggested by the previous work [12]. We consider both reconstructed future HOI features  $\hat{F}_{\text{seq}}^{\text{R}}[N_p+1:N_p+N_f]$  and anchored past counterparts  $\hat{F}_{\text{seq}}^{\text{R}}[0:N_p]$  compared to [12] as mentioned before. We also notice that the latent feature spaces before and after the denoising diffusion process represent the same “profile” of the input HOI sequence. Therefore, we propose an additional regularization term implicitly linking  $F_{\text{seq}}^{\text{R}}$  and  $\hat{F}_{\text{seq}}^{\text{R}}$  by hand trajectory prediction:

$$\mathcal{L}_{\text{reg}}^{\text{R}} = \sum_{t=1}^{N_f} \|\hat{H}_t^{\text{R}} - H_t^{\text{R},\text{gt}}\|^2, \quad (4)$$

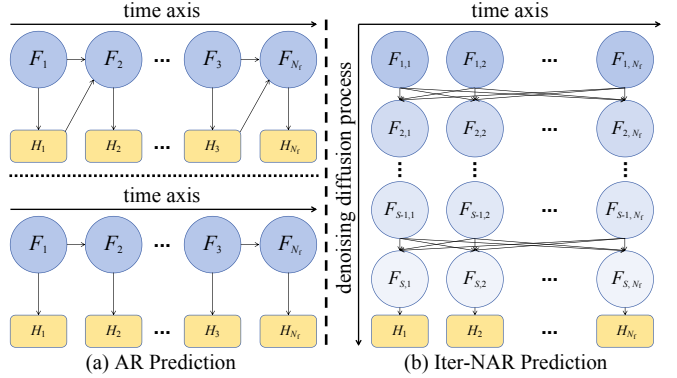


Fig. 4: Comparison of AR and our iter-NAR prediction.

where  $\hat{H}_t^{\text{R}} = f_{\text{HTH}}(F_{\text{seq}}^{\text{R}}[N_p+1:N_p+N_f])$ . Although Eq. (4) does not explicitly contain the term  $\hat{F}_{\text{seq}}^{\text{R}}$ , the training direction is the same with Eq. (2), thus maintaining training stability. The regularization helps distill HOI state knowledge by building a closer gradient connection constraining the two latent spaces alongside the diffusion process for better optimization. Here we do not use object affordance prediction for regularization because we empirically found that incorporating OAH mitigates training efficiency while the positive effect is not obvious. Finally, we get the total loss  $\mathcal{L}_{\text{total}}$ , the weighted sum of all the above-mentioned losses to train our proposed Diff-IP2D. Besides, we leverage the importance sampling technique proposed in improved DDPM [58], which promotes the training process focusing more on the steps with relatively large  $\mathcal{L}_{\text{total}}$ .

### D. Inference

In the inference stage, we first sample  $F_{\text{noise}}^{\text{R}}$ ,  $F_{\text{noise}}^{\text{L}} \in \mathbb{R}^{N_f \times a}$  from a standard Gaussian distribution, which is then concatenated with  $F_{\text{seq}}^{\text{R}}$ ,  $F_{\text{seq}}^{\text{L}} \in \mathbb{R}^{N_p \times a}$  along the time axis to generate  $\mathbf{z}_S^{\text{R}}$  and  $\mathbf{z}_S^{\text{L}}$ . Then we use MADT to predict  $\mathbf{z}_0^{\text{R}}$  and  $\mathbf{z}_0^{\text{L}}$  based on DDIM sampling [59]. Note that we anchor the past part of reparameterized  $\mathbf{z}_s$  as the fixed condition in every step of the inference process following Gong et al. [26]. Finally, the generated  $\hat{F}_{\text{seq}}^{\text{R}}$  and  $\hat{F}_{\text{seq}}^{\text{L}}$  are used to predict future hand waypoints and contact points by  $f_{\text{HTH}}(\cdot)$  and  $f_{\text{OAH}}(\cdot)$  as mentioned before. It can be seen from the inference stage that Diff-IP2D can be regarded as an iter-NAR model in the latent feature space.

**Takeaways.** Compared to the state-of-the-art baselines in an autoregressive manner, Diff-IP2D shifts the limited iterations along the time axis to sufficient iterations in the diffusion denoising direction, as shown in Fig. 4. This alleviates the accumulated artifacts caused by the limited iterations in the time dimension, and maintains bidirectional constraints (inherent in MADT) among the sequential features to generate future HOI states in parallel. Bidirectional constraints respect the fact that possible final HOI states also affect prior hand trajectories beyond temporal causality. We argue that this new paradigm provides a deeper understanding of high-level human intention for more accurate HOI prediction.

TABLE I: Comparison of performance on hand trajectory and object affordance prediction

approach	EK55			EK100			EG		
	WDE ↓	FDE ↓	WDE ↓						
CVH	0.636	0.315	0.658	0.329	0.689	0.343			
Seq2Seq [56]	0.505	0.212	0.556	0.219	0.649	0.263			
FHOI [14]	0.589	0.307	0.550	0.274	0.557	0.268			
OCT [12]	0.446	0.208	0.467	0.206	0.514	0.249			
USST [13]	0.458	0.210	0.475	0.206	0.552	0.256			
Diff-IP2D (ours)	<b>0.411</b>	<b>0.181</b>	<b>0.407</b>	<b>0.187</b>	<b>0.478</b>	<b>0.211</b>			
	SIM ↑	AUC-J ↑	NSS ↑	SIM ↑	AUC-J ↑	NSS ↑	SIM ↑	AUC-J ↑	NSS ↑
Center Object [14]	0.083	0.553	0.448	0.081	0.558	0.401	0.094	0.562	0.518
Hotspots [57]	0.156	0.670	0.606	0.147	0.635	0.533	0.150	0.662	0.574
FHOI [14]	0.159	0.655	0.517	0.120	0.548	0.418	0.122	0.506	0.401
OCT [12]	0.213	0.710	0.791	0.187	0.677	0.695	0.227	0.704	0.912
USST-FH [13]	0.208	0.682	0.757	0.179	0.658	0.754	0.190	0.675	0.729
Diff-IP2D (ours)	<b>0.226</b>	<b>0.725</b>	<b>0.980</b>	<b>0.211</b>	<b>0.736</b>	<b>0.917</b>	<b>0.242</b>	<b>0.722</b>	<b>0.956</b>
	SIM* ↑	AUC-J* ↑	NSS* ↑	SIM* ↑	AUC-J* ↑	NSS* ↑	SIM* ↑	AUC-J* ↑	NSS* ↑
FHOI [14]	0.130	0.602	0.487	0.113	0.545	0.409	0.118	0.501	0.379
OCT [12]	0.219	0.720	0.848	0.182	0.684	0.662	0.194	0.672	0.752
Diff-IP2D (ours)	<b>0.222</b>	<b>0.730</b>	<b>0.888</b>	<b>0.204</b>	<b>0.727</b>	<b>0.844</b>	<b>0.226</b>	<b>0.701</b>	<b>0.825</b>

## IV. EXPERIMENTS

### A. Experimental setups

**Datasets.** Following the previous work [12], we utilize three public datasets, Epic-Kitchens-55 (EK55) [60], Epic-Kitchens-100 (EK100) [61], and EGTEA Gaze+ (EG) [11]. For the EK55 and EK100 datasets, we sample past  $N_p = 10$  frames (2.5 s) to forecast HOI states in future  $N_f = 4$  frames (1.0 s), both at 4 FPS. As to the EG dataset,  $N_p = 9$  frames (1.5 s) are used for  $N_f = 3$  HOI predictions (0.5 s) at 6 FPS. All the training and test splits are obtained following [12].

**Diff-IP2D configuration.** MFE extracts the hand, object, and global feature vectors all with the size of 512 for each input image. For the EK55 and EK100 datasets, the outputs of SOFM  $F_{\text{seq}}^R$ ,  $F_{\text{seq}}^L$  have the size of  $14 \times 512$  for training and  $10 \times 512$  for inference. For the EG dataset,  $F_{\text{seq}}^R$ ,  $F_{\text{seq}}^L$  are  $9 \times 512$  for training and  $12 \times 512$  for inference. As to the diffusion process, the total number of steps  $S$  is set to 1000. The square-root noise schedule in Diffusion-LM [62] is adopted here for the forward diffusion process. MADT has 6 Transformer layers (Fig. 3) for denoising, where the embedding dimension is 512, the number of heads is set to 4, and the intermediate dimension of the feed-forward layer is set to 2048. Motion Encoder linearly projects each homography matrix to an egomotion feature vector of 512. We use an MLP with hidden dimensions 256 and 64 to predict the hand waypoints as HTH, and a C-VAE containing an MLP with a hidden dimension 512 to predict contact points as OAH. For training Diff-IP2D, we use AdamW optimizer [63] with a learning rate  $2e-4$ . All the modules are trained for 30 epochs with a batch size of 8 on 2 A100 GPUs. In the reference stage, we generate the 10 candidate samples for each prediction.

**Baseline configuration.** We choose Constant Velocity Hand (CVH), Seq2Seq [56], FHOI [14], OCT [12], and USST [13] as the baselines for hand trajectory prediction. CVH is the most straightforward one, which assumes two hands remain in uniform motion over the future time horizon with the average velocity during past observations. We choose Center Object [14], Hotspots [57], FHOI [14], OCT [12], and Final Hand of USST [13] (USST-FH) as the baselines for object affordance prediction. USST-FH puts a

mixture of Gaussians at the last hand waypoint predicted by USST since its vanilla version can only predict waypoints.

**Evaluation metrics.** Following the previous works [12]–[14], we use Final Displacement Error (FDE) to evaluate hand trajectory prediction performance. Considering the general knowledge of “post-contact trajectories” extracted from human videos is potentially beneficial to robot manipulation [1], [18], we additionally extend the metric Average Displacement Error to Weighted Displacement Error (WDE):

$$\text{WDE} = \frac{1}{2N_f} \sum_{R,L} \sum_{t=1}^{N_f} \frac{t}{N_f} D(H_t, H_t^{\text{gt}}), \quad (5)$$

where  $D(\cdot)$  denotes the L2 distance function and later waypoints contribute to larger errors. We select the mean error among the 10 samples for each trajectory prediction. As to object affordance prediction, we use Similarity Metric (SIM) [64], AUC-Judd (AUC-J) [65], and Normalized Scanpath Saliency (NSS) [66] as evaluation metrics. We use all 10 contact point candidates to compute them.

Moreover, we propose a novel object-centric protocol to jointly evaluate the two prediction tasks. We first calculate the averaged hand waypoints  $\bar{H}_t^R$  and  $\bar{H}_t^L$  for each future timestamp from multiple samples. Then we select the waypoint closest to each predicted contact prediction  $O_n$  as an additional “interaction point”, which can be formulated by:

$$\bar{H}_n^{\text{ip}} = \min_{R,L,t} D(\bar{H}_t, O_n). \quad (6)$$

Ultimately, the joint hotspot is predicted using  $\{\bar{H}_n^{\text{ip}} \cup O_n\}_{n=1}^{N_o}$ . This protocol comprehensively considers object-centric attention since HOI changes object states and hand waypoints must have a strong correlation with object positions. Note that we also use the quantitative metrics same as the ones for object affordance prediction, which are denoted as SIM\*, AUC-J\*, and NSS\*.

### B. Separate evaluation on hand trajectory and object affordance prediction

We first present the evaluation results on hand trajectory prediction. As Tab. I depicts, our proposed Diff-IP2D outperforms all the baselines on both EK55 and EK100 on WDE and FDE. This is mainly achieved by the devised iter-NAR paradigm of Diff-IP2D alleviating degeneration

TABLE II: Ablation study on egomotion guidance

approach	EK55					EK100				
	WDE ↓	FDE ↓	SIM ↑	AUC-J ↑	NSS ↑	WDE ↓	FDE ↓	SIM ↑	AUC-J ↑	NSS ↑
Diff-IP2D*	0.427	0.186	0.218	0.717	0.929	0.439	0.198	0.201	0.710	0.846
Diff-IP2D	<b>0.411</b>	<b>0.181</b>	<b>0.226</b>	<b>0.725</b>	<b>0.980</b>	<b>0.407</b>	<b>0.187</b>	<b>0.211</b>	<b>0.736</b>	<b>0.917</b>
improvement	3.7%	2.7%	3.7%	1.1%	5.5%	7.3%	5.6%	5.0%	3.7%	8.4%

Diff-IP2D\*: Diff-IP2D w/o egomotion guidance

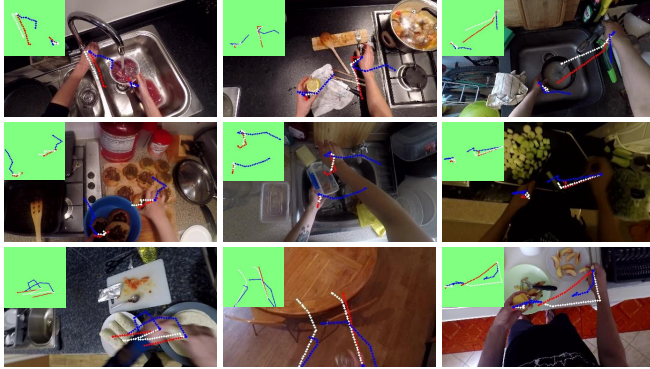


Fig. 5: Visualization of hand trajectory prediction on Epic-Kitchens. The waypoints from ground-truth, Diff-IP2D, and the second-best baseline [12] are connected by red, white, and blue dashed lines.

in AR baselines, as well as the egomotion guidance. The visualization of hand prediction results is shown in Fig. 5. It can be seen that our proposed method can better capture the camera wearer’s intention (such as putting the food in the bowl) and generate more reasonable future trajectories even if lacking past observations for hands (such as reaching out towards the table). Besides, our method can predict a good final hand position although there is a large shift in the early stage (the subfigure in the bottom right corner of Fig. 5), which benefits from our parallel generation with bidirectional constraints. When directly transferring the models trained on Epic-Kitchens to the unseen EG dataset, our method still outperforms the other baselines, improving by 7.0% and 15.3% against the second-best method on WDE and FDE respectively. This reveals the solid generalization capability of our Diff-IP2D across different environments.

The comparison results of object affordance prediction are also shown in Tab. I. Our proposed Diff-IP2D predicts the hotspots with larger SIM, AUC-J, and NSS compared to all the baselines on both Epic-Kitchens data and unseen EG data. Fig. 6 illustrates the predicted contact points with minimum distances to the ground-truth ones. Our proposed method focuses more on objects of interest considering the features of the holistic interaction and potential hand trajectories, and therefore grounds the contact points closer to the ground-truth labels than the counterparts of the baseline.

### C. Joint evaluation on hand-object interaction prediction

We further compare Diff-IP2D with the other two joint prediction baselines, FHOI [14] and OCT [12], using our proposed object-centric protocol. The video clips containing both ground-truth hand waypoints and contact points are used for evaluation in this experiment. The results are also shown in Tab. I, which indicates that our proposed Diff-IP2D can generate the best object-centric HOI predictions considering



Fig. 6: Visualization of object affordance prediction on Epic-Kitchens. The contact points from ground-truth, Diff-IP2D, and the state-of-the-art baseline OCT [12] are represented by red, white, and blue dots respectively. For a clearer illustration, we additionally put a fixed Gaussian with each contact point as the center.

the two tasks concurrently on both Epic-Kitchens and unseen EG data. The results also suggest that Diff-IP2D outperforms the baselines on object-centric HOI prediction by focusing more attention on the target objects and predicting reasonable hand trajectories around them.

### D. Ablation study on egomotion guidance

We provide an ablation study of the egomotion features used to guide MADT denoising on the EK55 and EK100 datasets. Here we replace the MHCA in MADT with a multi-head self-attention module (MHSA) to remove the egomotion guidance while keeping the same parameter number. The experimental results in Tab. II show that the guidance of motion features improves our proposed diffusion-based paradigm noticeably on both hand trajectory prediction and object affordance prediction. This is achieved by narrowing the two gaps caused by 2D-3D ill-posed problem and view difference mentioned in Sec. I. Note that the egomotion guidance is more significant on the EK100 dataset than on the EK55 dataset. The reason could be that EK100 has a larger volume of training data incorporating more diverse egomotion patterns than EK55, leading to a model that can capture human dynamics better.

## V. CONCLUSION AND INSIGHTS

In this paper, we propose a novel hand-object interaction prediction method Diff-IP2D. Specifically, we implement the devised denoising diffusion in the latent feature space under our proposed egomotion guidance, and jointly predict future hand trajectories and object affordances with the recovered latents on 2D egocentric videos. According to the experimental results, Diff-IP2D dominates the existing baselines on both off-the-shelf metrics and our new evaluation protocol, suggesting promising applications in artificial intelligence systems. It innovatively learns to recover latent HOI features

and forecast future HOI states in parallel with bidirectional constraints, which can serve as a foundation generative paradigm for future works on predictive tasks.

## REFERENCES

- [1] S. Bahl, R. Mendonca, L. Chen, U. Jain, and D. Pathak, “Affordances from human videos as a versatile representation for robotics,” in *Proceedings of the IEEE/CVF Conference on Computer Vision and Pattern Recognition*, pp. 13778–13790, 2023.
- [2] M. Chang, A. Prakash, and S. Gupta, “Look ma, no hands! agent-environment factorization of egocentric videos,” *arXiv preprint arXiv:2305.16301*, 2023.
- [3] S. Han, P.-c. Wu, Y. Zhang, B. Liu, L. Zhang, Z. Wang, W. Si, P. Zhang, Y. Cai, T. Hodan, *et al.*, “Umetrack: Unified multi-view end-to-end hand tracking for vr,” in *SIGGRAPH Asia 2022 Conference Papers*, pp. 1–9, 2022.
- [4] X. Xu, Y.-L. Li, and C. Lu, “Dynamic context removal: A general training strategy for robust models on video action predictive tasks,” *International Journal of Computer Vision*, vol. 131, no. 12, pp. 3272–3288, 2023.
- [5] Y.-D. Zheng, Z. Liu, T. Lu, and L. Wang, “Dynamic sampling networks for efficient action recognition in videos,” *IEEE Transactions on Image Processing*, vol. 29, pp. 7970–7983, 2020.
- [6] C. Zhang, C. Fu, S. Wang, N. Agarwal, K. Lee, C. Choi, and C. Sun, “Object-centric video representation for long-term action anticipation,” in *Proceedings of the IEEE/CVF Winter Conference on Applications of Computer Vision*, pp. 6751–6761, 2024.
- [7] Y.-D. Zheng, G. Chen, M. Yuan, and T. Lu, “Mrsn: Multi-relation support network for video action detection,” in *2023 IEEE International Conference on Multimedia and Expo (ICME)*, pp. 1026–1031, 2023.
- [8] M. Zhang, K. Teck Ma, J. Hwee Lim, Q. Zhao, and J. Feng, “Deep future gaze: Gaze anticipation on egocentric videos using adversarial networks,” in *Proceedings of the IEEE Conference on Computer Vision and Pattern Recognition*, pp. 4372–4381, 2017.
- [9] B. Lai, M. Liu, F. Ryan, and J. M. Rehg, “In the eye of transformer: Global-local correlation for egocentric gaze estimation and beyond,” *International Journal of Computer Vision*, vol. 132, no. 3, pp. 854–871, 2024.
- [10] Y. Li, A. Fathi, and J. M. Rehg, “Learning to predict gaze in egocentric video,” in *Proceedings of the IEEE International Conference on Computer Vision*, pp. 3216–3223, 2013.
- [11] Y. Li, M. Liu, and J. M. Rehg, “In the eye of beholder: Joint learning of gaze and actions in first person video,” in *Proceedings of the European Conference on Computer Vision (ECCV)*, pp. 619–635, 2018.
- [12] S. Liu, S. Tripathi, S. Majumdar, and X. Wang, “Joint hand motion and interaction hotspots prediction from egocentric videos,” in *Proceedings of the IEEE/CVF Conference on Computer Vision and Pattern Recognition*, pp. 3282–3292, 2022.
- [13] W. Bao, L. Chen, L. Zeng, Z. Li, Y. Xu, J. Yuan, and Y. Kong, “Uncertainty-aware state space transformer for egocentric 3d hand trajectory forecasting,” in *Proceedings of the IEEE/CVF International Conference on Computer Vision*, pp. 13702–13711, 2023.
- [14] M. Liu, S. Tang, Y. Li, and J. M. Rehg, “Forecasting human-object interaction: joint prediction of motor attention and actions in first person video,” in *Proceedings of the European Conference on Computer Vision (ECCV)*, pp. 704–721, 2020.
- [15] D. Shan, J. Geng, M. Shu, and D. F. Fouhey, “Understanding human hands in contact at internet scale,” in *Proceedings of the IEEE/CVF Conference on Computer Vision and Pattern Recognition*, pp. 9869–9878, 2020.
- [16] Y. Ye, X. Li, A. Gupta, S. De Mello, S. Birchfield, J. Song, S. Tulsiani, and S. Liu, “Affordance diffusion: Synthesizing hand-object interactions,” in *Proceedings of the IEEE/CVF Conference on Computer Vision and Pattern Recognition*, pp. 22479–22489, 2023.
- [17] S. Xu, Z. Li, Y.-X. Wang, and L.-Y. Gui, “Interdiff: Generating 3d human-object interactions with physics-informed diffusion,” in *Proceedings of the IEEE/CVF International Conference on Computer Vision*, pp. 14928–14940, 2023.
- [18] R. Mendonca, S. Bahl, and D. Pathak, “Structured world models from human videos,” *arXiv preprint arXiv:2308.10901*, 2023.
- [19] S. Bahl, A. Gupta, and D. Pathak, “Human-to-robot imitation in the wild,” *arXiv preprint arXiv:2207.09450*, 2022.
- [20] J. Ho, A. Jain, and P. Abbeel, “Denoising diffusion probabilistic models,” *Advances in Neural Information Processing Systems*, vol. 33, pp. 6840–6851, 2020.
- [21] P. Dhariwal and A. Nichol, “Diffusion models beat gans on image synthesis,” *Advances in Neural Information Processing Systems*, vol. 34, pp. 8780–8794, 2021.
- [22] P. Esser, J. Chiu, P. Atighehchian, J. Granskog, and A. Germanidis, “Structure and content-guided video synthesis with diffusion models,” in *Proceedings of the IEEE/CVF International Conference on Computer Vision*, pp. 7346–7356, 2023.
- [23] Y. Ji, Z. Chen, E. Xie, L. Hong, X. Liu, Z. Liu, T. Lu, Z. Li, and P. Luo, “Ddp: Diffusion model for dense visual prediction,” in *Proceedings of the IEEE/CVF International Conference on Computer Vision*, pp. 21741–21752, 2023.
- [24] J. Liu, G. Wang, W. Ye, C. Jiang, J. Han, Z. Liu, G. Zhang, D. Du, and H. Wang, “Diffflow3d: Toward robust uncertainty-aware scene flow estimation with diffusion model,” *arXiv preprint arXiv:2311.17456*, 2023.
- [25] W. Peebles and S. Xie, “Scalable diffusion models with transformers,” in *Proceedings of the IEEE/CVF International Conference on Computer Vision*, pp. 4195–4205, 2023.
- [26] S. Gong, M. Li, J. Feng, Z. Wu, and L. Kong, “Diffuseq: Sequence to sequence text generation with diffusion models,” in *International Conference on Learning Representations*, 2023.
- [27] S. Gong, M. Li, J. Feng, Z. Wu, and L. Kong, “Diffuseq-v2: Bridging discrete and continuous text spaces for accelerated seq2seq diffusion models,” *arXiv preprint arXiv:2310.05793*, 2023.
- [28] A. Calway, W. Mayol-Cuevas, D. Damen, O. Haines, and T. Lee-lasawassuk, “Discovering task relevant objects and their modes of interaction from multi-user egocentric video,” in *British Machine Vision Conference*, 2015.
- [29] Y. Liu, P. Wei, and S.-C. Zhu, “Jointly recognizing object fluents and tasks in egocentric videos,” in *Proceedings of the IEEE International Conference on Computer Vision (ICCV)*, 2017.
- [30] M. Schroder and H. Ritter, “Hand-object interaction detection with fully convolutional networks,” in *Proceedings of the IEEE Conference on Computer Vision and Pattern Recognition Workshops*, pp. 18–25, 2017.
- [31] A. Darkhalil, D. Shan, B. Zhu, J. Ma, A. Kar, R. Higgins, S. Fidler, D. Fouhey, and D. Damen, “Epic-kitchens visor benchmark: Video segmentations and object relations,” *Advances in Neural Information Processing Systems*, vol. 35, pp. 13745–13758, 2022.
- [32] L. Zhang, S. Zhou, S. Stent, and J. Shi, “Fine-grained egocentric hand-object segmentation: Dataset, model, and applications,” in *Proceedings of the European Conference on Computer Vision*, pp. 127–145, 2022.
- [33] R. E. L. Higgins and D. F. Fouhey, “Moves: Manipulated objects in video enable segmentation,” in *Proceedings of the IEEE/CVF Conference on Computer Vision and Pattern Recognition (CVPR)*, pp. 6334–6343, June 2023.
- [34] A. Furnari and G. M. Farinella, “Rolling-unrolling lstms for action anticipation from first-person video,” *IEEE Transactions on Pattern Analysis and Machine Intelligence*, vol. 43, no. 11, pp. 4021–4036, 2020.
- [35] H. Fan, T. Zhuo, X. Yu, Y. Yang, and M. Kankanhalli, “Understanding atomic hand-object interaction with human intention,” *IEEE Transactions on Circuits and Systems for Video Technology*, vol. 32, no. 1, pp. 275–285, 2021.
- [36] T. Shiota, M. Takagi, K. Kumagai, H. Seshimo, and Y. Aono, “Egocentric action recognition by capturing hand-object contact and object state,” in *Proceedings of the IEEE/CVF Winter Conference on Applications of Computer Vision (WACV)*, pp. 6541–6551, January 2024.
- [37] J. Romero, D. Tzionas, and M. J. Black, “Embodied hands: Modeling and capturing hands and bodies together,” *arXiv preprint arXiv:2201.02610*, 2022.
- [38] Y. Zhou, M. Habermann, W. Xu, I. Habibie, C. Theobalt, and F. Xu, “Monocular real-time hand shape and motion capture using multi-modal data,” in *Proceedings of the IEEE/CVF Conference on Computer Vision and Pattern Recognition*, pp. 5346–5355, 2020.
- [39] Z. Lin, C. Ding, H. Yao, Z. Kuang, and S. Huang, “Harmonious feature learning for interactive hand-object pose estimation,” in *Proceedings of the IEEE/CVF Conference on Computer Vision and Pattern Recognition (CVPR)*, pp. 12989–12998, June 2023.
- [40] L. Yang, K. Li, X. Zhan, J. Lv, W. Xu, J. Li, and C. Lu, “Artiboost: Boosting articulated 3d hand-object pose estimation via online explo-

ration and synthesis,” in *Proceedings of the IEEE/CVF Conference on Computer Vision and Pattern Recognition*, pp. 2750–2760, 2022.

[41] S. Liu, H. Jiang, J. Xu, S. Liu, and X. Wang, “Semi-supervised 3d hand-object poses estimation with interactions in time,” in *Proceedings of the IEEE/CVF Conference on Computer Vision and Pattern Recognition*, pp. 14687–14697, 2021.

[42] J. J. Lim, H. Pirsiavash, and A. Torralba, “Parsing ikea objects: Fine pose estimation,” in *Proceedings of the IEEE International Conference on Computer Vision*, pp. 2992–2999, 2013.

[43] K. Grauman, A. Westbury, E. Byrne, Z. Chavis, A. Furnari, R. Girdhar, J. Hamburger, H. Jiang, M. Liu, X. Liu, *et al.*, “Ego4d: Around the world in 3,000 hours of egocentric video,” in *Proceedings of the IEEE/CVF Conference on Computer Vision and Pattern Recognition*, pp. 18995–19012, 2022.

[44] H. Bharadhwaj, A. Gupta, V. Kumar, and S. Tulsiani, “Towards generalizable zero-shot manipulation via translating human interaction plans,” *arXiv preprint arXiv:2312.00775*, 2023.

[45] E. Dessalene, C. Devaraj, M. Maynord, C. Fermüller, and Y. Aloimonos, “Forecasting action through contact representations from first person video,” *IEEE Transactions on Pattern Analysis and Machine Intelligence*, vol. 45, no. 6, pp. 6703–6714, 2023.

[46] M. Luo, Z. Xue, A. Dimakis, and K. Grauman, “Put myself in your shoes: Lifting the egocentric perspective from exocentric videos,” *arXiv preprint arXiv:2403.06351*, 2024.

[47] S. Zhang, Q. Ma, Y. Zhang, S. Aliakbarian, D. Cosker, and S. Tang, “Probabilistic human mesh recovery in 3d scenes from egocentric views,” in *Proceedings of the IEEE/CVF International Conference on Computer Vision*, pp. 7989–8000, 2023.

[48] Y. Liu, J. Yang, X. Gu, Y. Guo, and G.-Z. Yang, “EgoHMR: Egocentric human mesh recovery via hierarchical latent diffusion model,” in *2023 IEEE International Conference on Robotics and Automation (ICRA)*, pp. 9807–9813, 2023.

[49] Y. Ye, P. Hebbar, A. Gupta, and S. Tulsiani, “Diffusion-guided reconstruction of everyday hand-object interaction clips,” in *Proceedings of the IEEE/CVF International Conference on Computer Vision (ICCV)*, pp. 19717–19728, October 2023.

[50] Z. Zhu and D. Damen, “Get a grip: Reconstructing hand-object stable grasps in egocentric videos,” *arXiv preprint arXiv:2312.15719*, 2023.

[51] M. Zhang, Y. Fu, Z. Ding, S. Liu, Z. Tu, and X. Wang, “Hoidiffusion: Generating realistic 3d hand-object interaction data,” *arXiv preprint arXiv:2403.12011*, 2024.

[52] K. He, G. Gkioxari, P. Dollár, and R. Girshick, “Mask r-cnn,” in *Proceedings of the IEEE International Conference on Computer Vision*, pp. 2961–2969, 2017.

[53] D. G. Lowe, “Distinctive image features from scale-invariant keypoints,” *International journal of computer vision*, vol. 60, pp. 91–110, 2004.

[54] M. A. Fischler and R. C. Bolles, “Random sample consensus: a paradigm for model fitting with applications to image analysis and automated cartography,” *Communications of the ACM*, vol. 24, no. 6, pp. 381–395, 1981.

[55] K. Sohn, H. Lee, and X. Yan, “Learning structured output representation using deep conditional generative models,” *Advances in Neural Information Processing Systems*, vol. 28, 2015.

[56] I. Sutskever, O. Vinyals, and Q. V. Le, “Sequence to sequence learning with neural networks,” *Advances in Neural Information Processing Systems*, vol. 27, 2014.

[57] T. Nagarajan, C. Feichtenhofer, and K. Grauman, “Grounded human-object interaction hotspots from video,” in *Proceedings of the IEEE/CVF International Conference on Computer Vision*, pp. 8688–8697, 2019.

[58] A. Q. Nichol and P. Dhariwal, “Improved denoising diffusion probabilistic models,” in *International Conference on Machine Learning*, pp. 8162–8171, 2021.

[59] J. Song, C. Meng, and S. Ermon, “Denoising diffusion implicit models,” *arXiv preprint arXiv:2010.02502*, 2020.

[60] D. Damen, H. Doughty, G. M. Farinella, S. Fidler, A. Furnari, E. Kazakos, D. Moltisanti, J. Munro, T. Perrett, W. Price, *et al.*, “Scaling egocentric vision: The epic-kitchens dataset,” in *Proceedings of the European Conference on Computer Vision (ECCV)*, pp. 720–736, 2018.

[61] D. Damen, H. Doughty, G. M. Farinella, A. Furnari, E. Kazakos, J. Ma, D. Moltisanti, J. Munro, T. Perrett, W. Price, *et al.*, “Rescaling egocentric vision: Collection, pipeline and challenges for epic-kitchens-100,” *International Journal of Computer Vision*, pp. 1–23, 2022.

[62] X. Li, J. Thickstun, I. Gulrajani, P. S. Liang, and T. B. Hashimoto, “Diffusion-lm improves controllable text generation,” *Advances in Neural Information Processing Systems*, vol. 35, pp. 4328–4343, 2022.

[63] D. P. Kingma and J. Ba, “Adam: A method for stochastic optimization,” *arXiv preprint arXiv:1412.6980*, 2014.

[64] M. J. Swain and D. H. Ballard, “Color indexing,” *International Journal of Computer Vision*, vol. 7, no. 1, pp. 11–32, 1991.

[65] T. Judd, K. Ehinger, F. Durand, and A. Torralba, “Learning to predict where humans look,” in *Proceedings of the IEEE International Conference on Computer Vision*, pp. 2106–2113, 2009.

[66] R. J. Peters, A. Iyer, L. Itti, and C. Koch, “Components of bottom-up gaze allocation in natural images,” *Vision Research*, vol. 45, no. 18, pp. 2397–2416, 2005.